2021

The Stability of Two-Dimensional Cylinder Wakes in the Presence of a Wavy Ground

Matt Duran
University of Central Florida

THE STABILITY OF TWO-DIMENSIONAL CYLINDER WAKES IN THE PRESENCE OF A WAVY GROUND

by

MATT DURAN

A thesis submitted in partial fulfillment of the requirements
for the Honors in the Major Program in Mechanical Engineering
in the College of Engineering and Computer Science
and in The Burnett Honors College
at the University of Central Florida
Orlando, Florida

Spring Term 2021

Thesis Chair: Dr. Samik Bhattacharya

ABSTRACT

The following study investigates hydrodynamic stability for two-dimensional, incompressible flow past a cylinder and compares it alongside four different variations of a wave-like ground introduced within the wake region of the cylinder wake. These different variations include changing the distance of the cylinder both horizontally from the wave-like structure and vertically from the ground. The geometry and meshes were initially constructed using GMSH and imported into Nektar++. The baseflows were then obtained in Nektar++ using the Velocity Correction Scheme, continuous Galerkin method, and Unsteady Navier Stokes solver. Then, the Implicitly Restarted Arnoldi Method driver was used to retrieve the various eigenvalues/eigenmodes and growth rates. Finally, the results were visualized in Paraview which allowed clear comparisons between the stability of the flow between each case. The findings obtained show a clear effect on stability when considering different cases, for a plain cylinder and for each case there are observations to be made in how the various eigenmodes varied in terms of magnitude and shape, other observations were made in the differing critical Reynolds number and frequencies among the cases. This study is relevant to various natural environments where a blunt object may come in range of a bumpy or wavy ground. In these scenarios it can be important to monitor how instabilities propagate and cause effects such as turbulence or drag. Additionally, investigation like these can detail how to effectively avoid undesirable characteristics of instability.

TABLE OF CONTENTS

LIST OF FIGURES

LIST OF TABLES

INTRODUCTION

Background

The analysis of the stability of fluids, also known as hydrodynamic stability, has long been studied in detail for a large range of scenarios and conditions. This may include confined flows such as Poiseuille flow show in **Error! Reference source not found.**and similar to in the study (Yuan et al., 2020) or unconfined flows such as flow past a cylinder which is the focus of this study.

Figure 1- Diagram of Poiseuille flow velocity profile confined by a circular channel

Hydrodynamic stability in general is highly relevant in the fields of aerodynamics, atmospheric sciences, astrophysics, chemistry, and biology. This is because of the prevalence of fluids in these fields and its chaotic nature which often leads to turbulence. If the flow is unstable then it is pertinent to study the conditions for instability and how different disturbances

may propagate throughout the flow. This is usually considered undesirable; instabilities and turbulence can lead to significant drag or noise thus it is important to prevent or consider how unstable the flow is.

For this study, hydrodynamic stability will be analyzed for the case of a cylinder wake and then analyzed when introducing several variations featuring the presence of a wave-like ground beneath. Temporal stability will be conducted using Nektar++ (Cantwell et al., 2015) to return and visualize the corresponding growth rates and eigenmodes of the flows in question. Finally, the results will be compared and visualized in ParaView with the plain case of a cylinder wake and the several wave-like ground conditions.

METHODS

Geometry/Meshing

To start, the geometry and meshes were created using GMSH version 4.8.0 and the built-in OpenCASCADE kernel. The main reason for using GMSH is that in can produce higher order meshes, all meshes used in this study were second order. In addition, Nektar++ is intended to primarily be used with GMSH meshes. The geometry and meshes to create include plain flow past a cylinder (Figure 3- Mesh for plain flow past a cylinder) and 4 different cases featuring a wave-like ground protruding from the floor below the cylinder. Moreover, the cases vary by distance both vertically and horizontally between the cylinder from the wave-like ground, a full diagram of this can be seen in Figure 2- Geometry of flow past a cylinder with a wave-like ground in case 1 The variable L is specifically the distance horizontally from the center of the cylinder to the left boundary of the wave-like structure denoted by P and marked in green, a negative sign denotes the distance L being behind the wave boundary and a positive L denotes the cylinder being to the right of the wave boundary P. The variable H refers to the vertical height from the center of the cylinder to the flat ground itself. The symbol λ denotes the wavelength of the wave structure while the symbol A denotes the amplitude where λ and A are 4D and 0.5D respectively for this study.

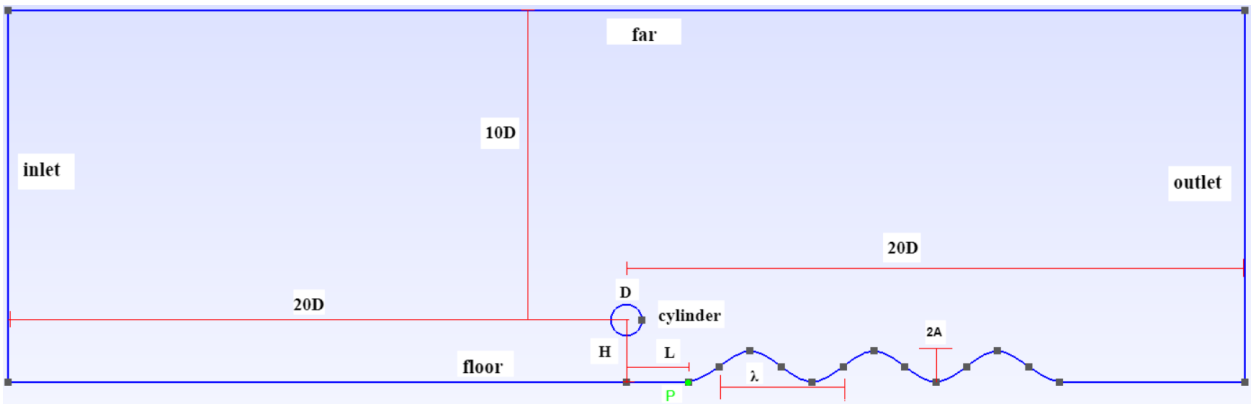

Figure 2- Geometry of flow past a cylinder with a wave-like ground in case 1

As seen in Table 1- Wave-like ground mesh cases 1- below, the distances were nondimensionalized in terms of the cylinder diameter D for each case being considered using the ratios L/D and H/D. Furthermore, the mesh for each case in the table is presented in Figure 4- Mesh for case 1

Table 1- Wave-like ground mesh cases 1-4

Case	Position of cylinder with respect to point P
1	L/D = -2, H/D = 2.5
2	L/D = 2, H/D = 2.5
3	L/D = 6, H/D = 2.5
4	L/D = -2, H/D = 1

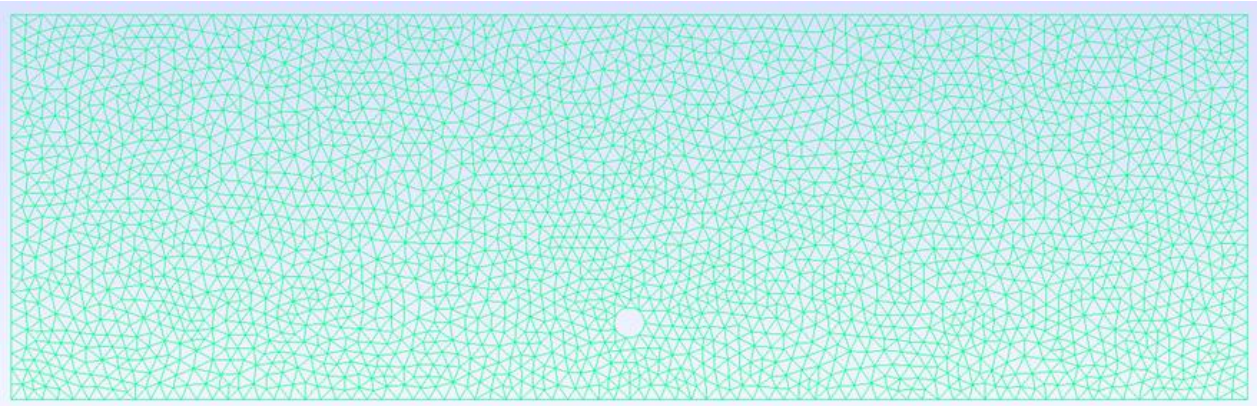

Figure 3- Mesh for plain flow past a cylinder

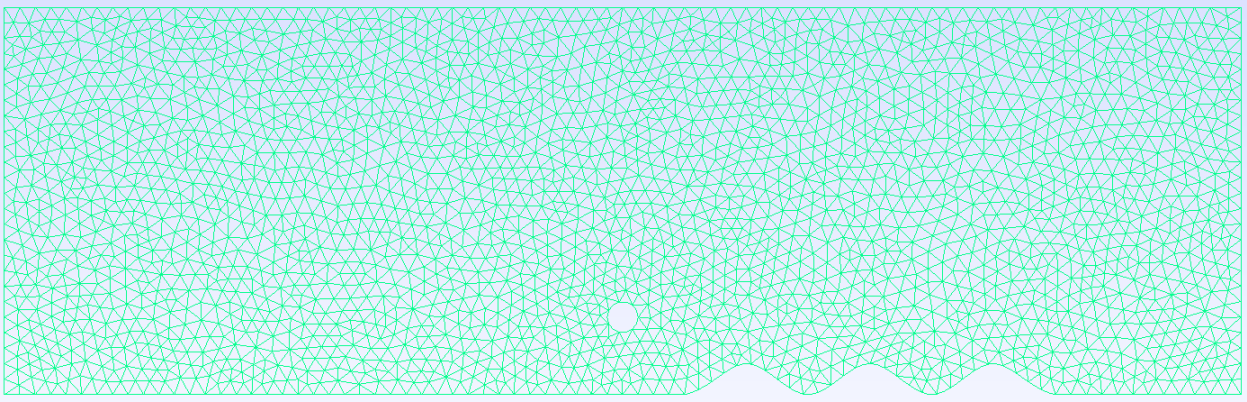

Figure 4- Mesh for case 1

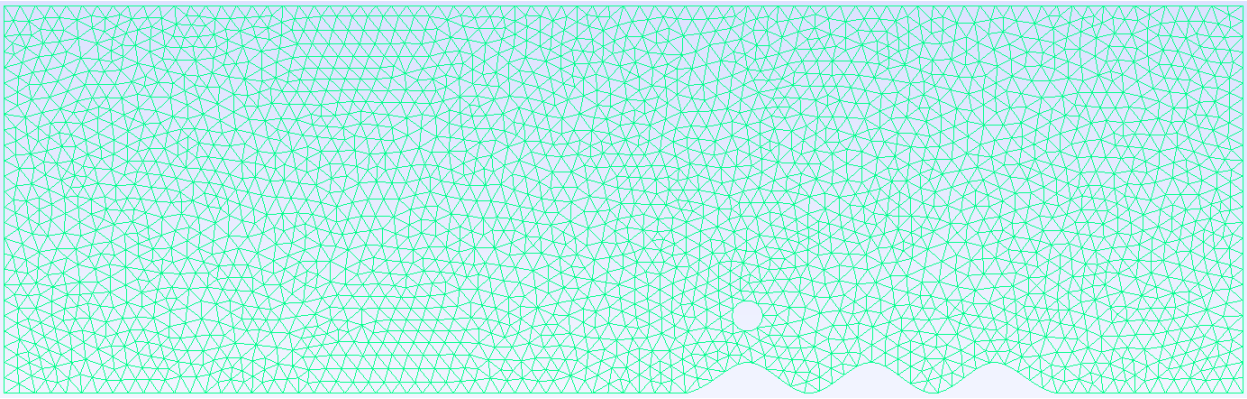

Figure 5- Mesh for case 2

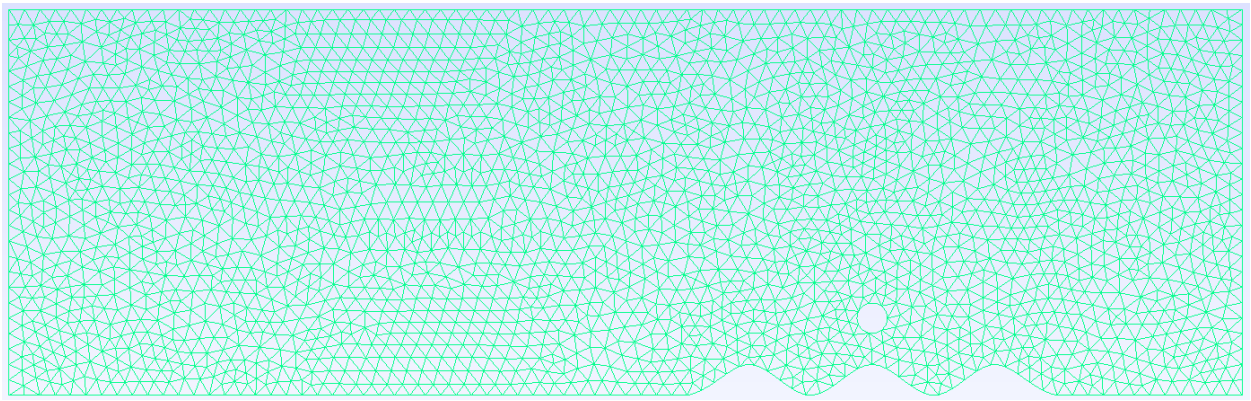

Figure 6- Mesh for case 3

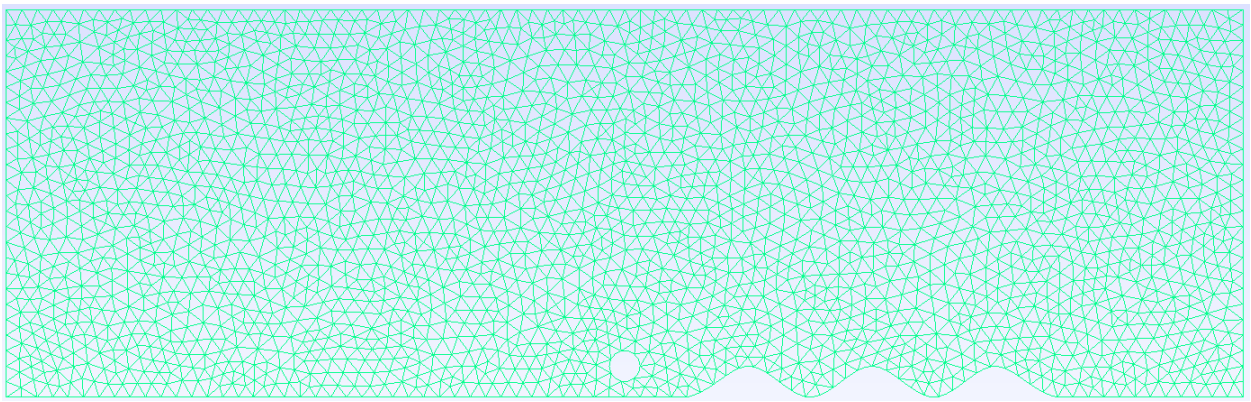

Figure 7- Mesh for case 4

Fluid simulations

For stability and computational fluid dynamics in general, Nektar++ version 5.0 was used in conjunction with the previous GMSH created meshes to simulate fluid dynamics for each case. The first step is to import the mesh into Nektar++ and convert it using the NekMesh feature so that it can utilized in Nektar++. Next, the solver settings are completed to specify things such as the scheme, equation type, and time integration method (Figure 8). The parameters are also filled in to specify the time step for the simulation and for how long the simulation will run, additionally the Reynolds number and kinematic viscosity are specified here (Figure 8). After this, the boundary regions and conditions need to be set up to specify the physics for the different areas of the mesh such as which portion is an inlet, outlet, or wall as well as the velocity and pressure for these regions (Figure 9).

```
      <CONDITIONS>
  <SOLVERINFO>
        <I PROPERTY="SolverType"             VALUE="VelocityCorrectionScheme"/>
        <I PROPERTY="TimeIntegrationMethod"  VALUE="IMEXOrder2"              />
        <I PROPERTY="EQTYPE"                 VALUE="UnsteadyNavierStokes"    />
        <I PROPERTY="EvolutionOperator"      VALUE="Nonlinear"               />
        <I PROPERTY="Projection"             VALUE="Continuous"              />
        <I PROPERTY="Driver"                 VALUE="Standard"                />
</SOLVERINFO>

  <PARAMETERS>
    <P> TimeStep      = 0.001     </P>
    <P> NumSteps      = 100000      </P>
    <P> IO_CheckSteps = 1000      </P>
    <P> IO_InfoSteps  = 1000        </P>
    <P> Re            = 25        </P>
    <P> Kinvis        = 1./Re     </P>
  </PARAMETERS>
```

Figure 8- case 1 solver settings and parameters for running simulations

```
<BOUNDARYREGIONS>
  <B ID="0"> C[1] </B> <!-- inlet     -->
  <B ID="1"> C[2] </B> <!-- outlet -->
  <B ID="2"> C[3] </B> <!-- floor -->
  <B ID="3"> C[4] </B> <!-- symmetry -->
  <B ID="4"> C[5] </B> <!-- cylinder -->
</BOUNDARYREGIONS>

<BOUNDARYCONDITIONS>
  <REGION REF="0">
    <D VAR="u" VALUE="1" />
    <D VAR="v" VALUE="0" />
    <N VAR="p" USERDEFINEDTYPE="H" VALUE="0"/>
  </REGION>
  <REGION REF="1">
    <N VAR="u" VALUE="0" />
    <N VAR="v" VALUE="0" />
    <D VAR="p" VALUE="0"/>
  </REGION>
  <REGION REF="2">
    <D VAR="u" VALUE="0" />
    <D VAR="v" VALUE="0" />
    <N VAR="p" USERDEFINEDTYPE="H" VALUE="0"/>
  </REGION>
  <REGION REF="3">
    <D VAR="u" VALUE="1" />
    <D VAR="v" VALUE="0" />
    <N VAR="p" USERDEFINEDTYPE="H" VALUE="0"/>
  </REGION>
<REGION REF="4">
    <D VAR="u" VALUE="0" />
    <D VAR="v" VALUE="0" />
    <N VAR="p" USERDEFINEDTYPE="H" VALUE="0"/>
  </REGION>
</BOUNDARYCONDITIONS>
```

Figure 9- case 1 defining boundary regions and conditions for running simulations

Comparison at uniform conditions

For the case of the base flow, the conditions will not be the same since to be at the critical state and the cases will be at a different Reynolds number. Therefore, it is useful to run a simulation for each case under uniform conditions to compare the different characteristics of the flow. For this study, a Reynolds number of 100 and a total simulation time of 50 seconds was chosen to clearly illustrate vortex shedding in each case which would not be present for the baseflow.

Base flow

As is standard in analyzing hydrodynamic stability, the baseflow must be obtained for each case which was determined for this study by running various simulations until the critical conditions are pin pointed. More specifically, for each individual case the simulation was ran at a certain Reynolds number where the flow was unstable and would continuously oscillate through time. Then, a lower Reynolds number simulation was simulated at which the flow would become stable and would be completely steady after enough time, this steady state would be verified by taking the velocity profile at different areas of the simulation and making sure it would not change with time. Finally, the Reynolds number would again be increased until it was just before an unstable state. These results would be used as the baseflow for later the running stability analysis for each case.

Stability

The main reason in selecting Nektar++ as the CFD package of chose is that it includes features to greatly facilitate stability. Conducting global stability is very difficult, other methods consist usually of modifying the source code of some other CFD package such as OpenFOAM to solve for the eigenvalues of the relevant stability equations, Nektar++ was consequentially chosen. When running a stability simulation in Nektar++ the main differences involve changing the solver and parameter info. This includes changing the driver to stability mode which in this case meant switching from standard to arpack and changing the time settings. For stability, this time refers to how long is spent on each iteration to solve for the eigenvalues. Additionally, the kyrlov space (*kdim*) determines how many eigenvalues are being solved for, this value may need

to be adjusted for each simulation. Next, the number of eigenvectors to converge and be returned is controlled by *nvec* and this tolerance for convergence is the *evtol* value.

Putting it all together, Figure 11 illustrates the steps taken from creating the mesh and inputting the Reynolds number for each simulation, to conducting stability analysis by using an eigenvalue solver and subsequentially retrieving eigenmodes to be visualized later. This process was repeated for each mesh and produced the results in the next section.

```
<SOLVERINFO>
        <I PROPERTY="SOLVERTYPE"              VALUE="VelocityCorrectionScheme"/>
        <I PROPERTY="EQTYPE"                  VALUE="UnsteadyNavierStokes"    />
        <I PROPERTY="EvolutionOperator"       VALUE="Direct"                  />
        <I PROPERTY="Projection"              VALUE="Galerkin"                />
        <I PROPERTY="TimeIntegrationMethod"   VALUE="IMEXOrder2"              />
        <I PROPERTY="Driver"                  VALUE="Arpack"                  />
        <I PROPERTY="ArpackProblemType"       VALUE="LargestMag"              />
</SOLVERINFO>

  <PARAMETERS>
    <P> TimeStep      = 0.001     </P>
    <P> NumSteps      = 500      </P>
    <P> IO_CheckSteps = 500       </P>
    <P> IO_InfoSteps  = 500         </P>
    <P> Re            = 25        </P>
    <P> Kinvis        = 1./Re     </P>
    <p> kdim          = 10                    </p>
    <P> nvec          = 4         </P>
    <P> evtol         = 1e-4      </P>
  </PARAMETERS>
```

Figure 10- Case 1 stability solver and parameter configuration

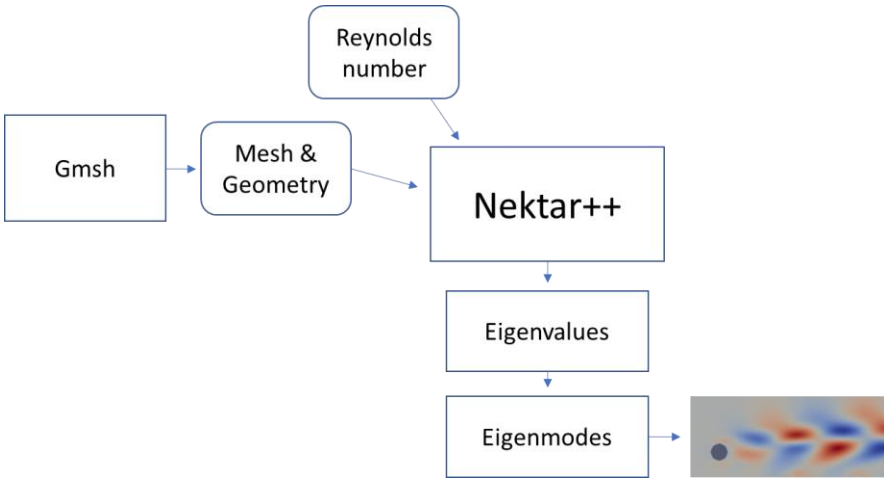

Figure 11- CFD methodology diagram

RESULTS

Comparison at *Re* = 100 contours

Below in Figure 12 the contours of the streamwise velocity can be seen. Vortex shedding can clearly be seen for flow past a cylinder and cases 1-3. For flow past a cylinder and case 1 the vortex shedding alternates and is characterized by the Von Karman street. Cases 2 and 3 however only contain the upper half of the Von Karman street as the wake meets the wavy ground. Finally, case 4 produced interesting results, the wake is still oscillating but there is no visible vortex in the flow.

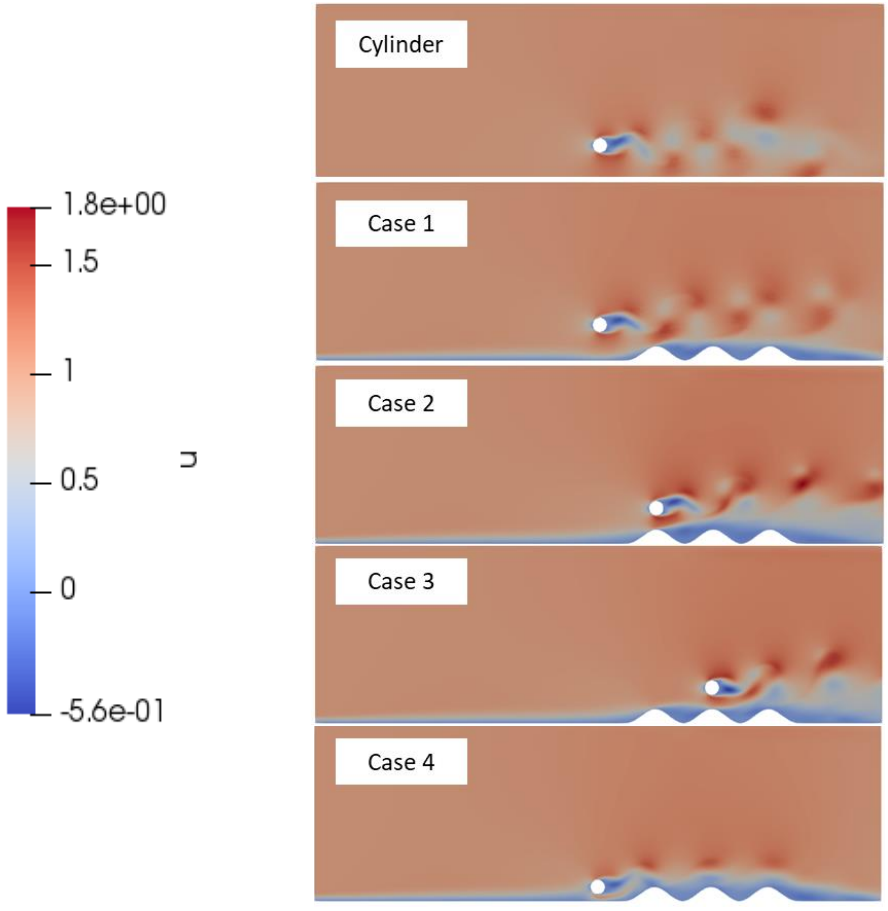

Figure 12- Contours of streamwise velocity (u) at *Re* = 100

From the previous results at *Re* = 100, the vorticity contour plot is show for the cylinder and cases 1-4. The results again show vortex shedding which alternates in terms of positive and negative vorticity. Except for case 4, the vorticity contours confirm that no vortex shedding is present and that the positive vorticity remains only near the cylinder.

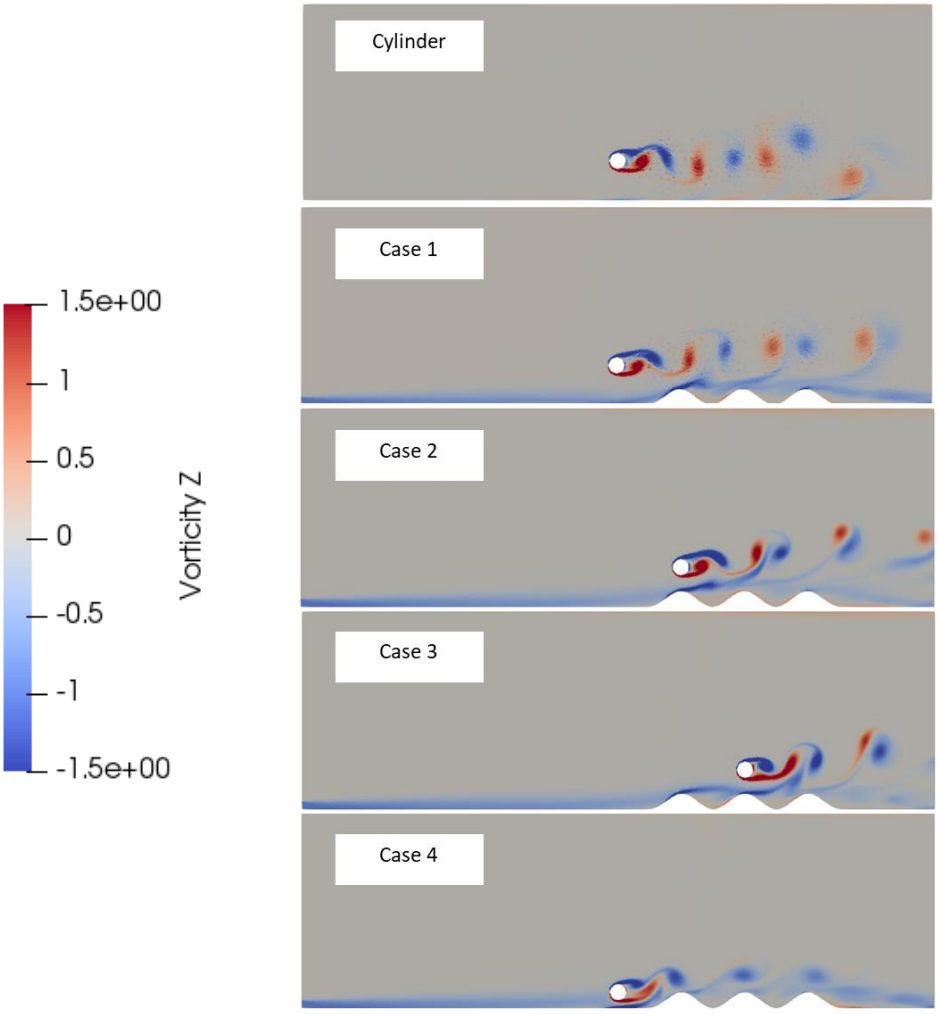

Figure 13- Contours of vorticity at *Re* = 100

Baseflow contours

The contours for the streamwise velocity for the obtained baseflows are shown below in Figure 14. For these configurations, the flow is considered approximately stable and will not have any significant changes with time. The first observation to be made is that they flow past the cylinder for this set up has critical Reynolds number of 30, cases 1-3 have values that are lower for the critical Reynolds number while case 4 has a value higher than all other cases. In addition, cases 2 and 3 appear similar in terms of velocity profiles and wakes.

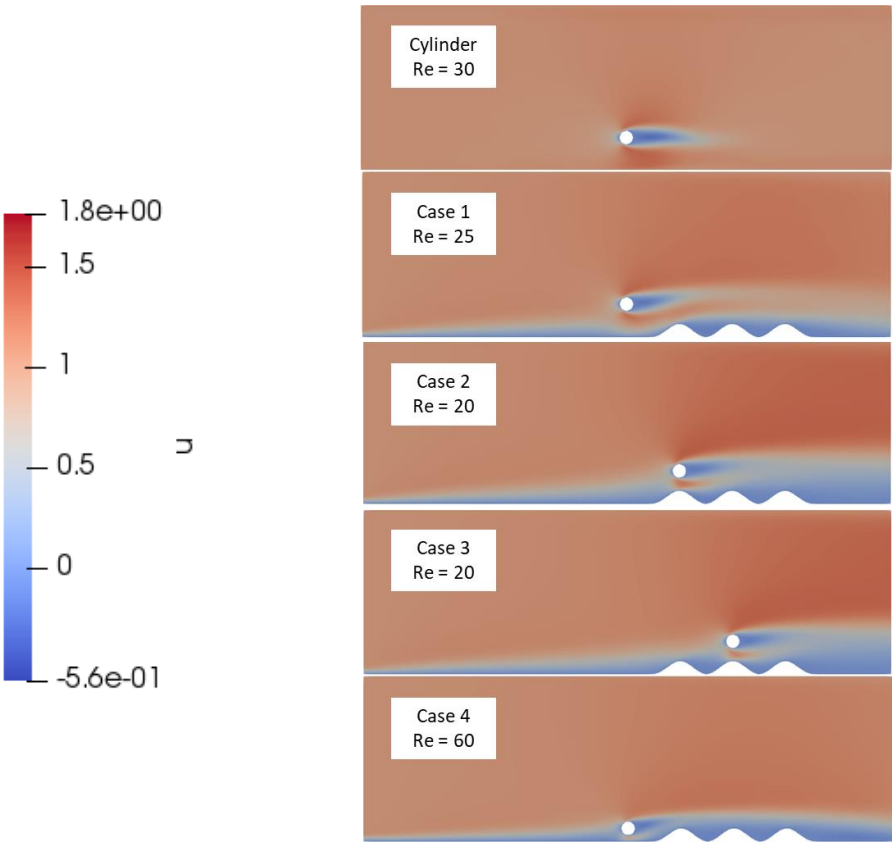

Figure 14- Contours of streamwise (u) velocity for the baseflow

The vorticity contour plot for the baseflow is now show in Figure 15 below. The plot shows clearly that no vortexes are present and that the positive vorticity remains near the cylinder. Additionally, cases 1-3 show similar wakes and patterns of negative vorticity arising as the flow meets and proceeds past the wavy ground.

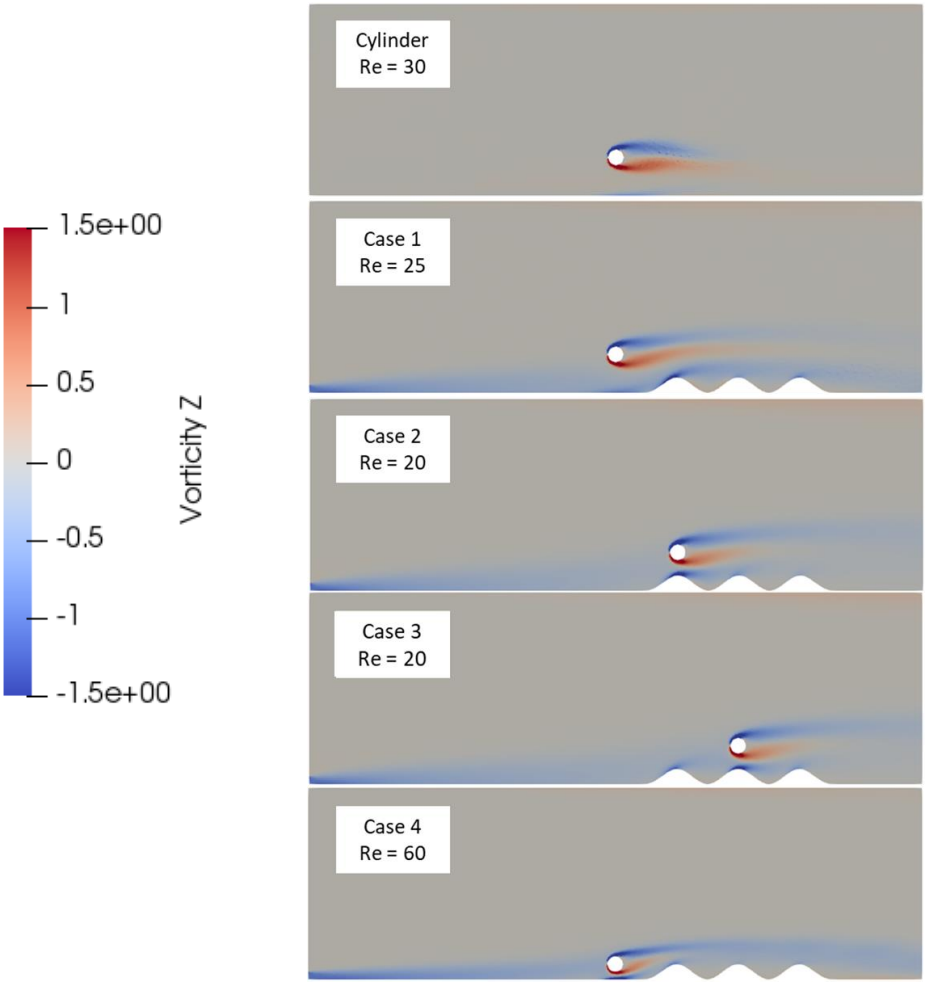

Figure 15- Contours of vorticity for the baseflow

Baseflow velocity profiles

In the following section, a velocity profile will be described by the variables u/u_{max} and *y/D* which are respectively the ratio of the velocity to maximum velocity and the ratio of the vertical coordinate to the diameter of the cylinder. These velocity profiles will extend to *y/D* 1 to 5 and be taken horizontally at a distance x from the center of the cylinder for each case. Then at the ratios *x/D* = 4, 8, 12 the velocity profiles will be recorded and plotted, this location will change for some cases as the distance is specifically from the center of the cylinder and the location of the cylinder varies. Figure 16 below is a diagram of the velocity profiles specifically for case 1, Figure 17 shows a similar diagram featuring cases 1-4.

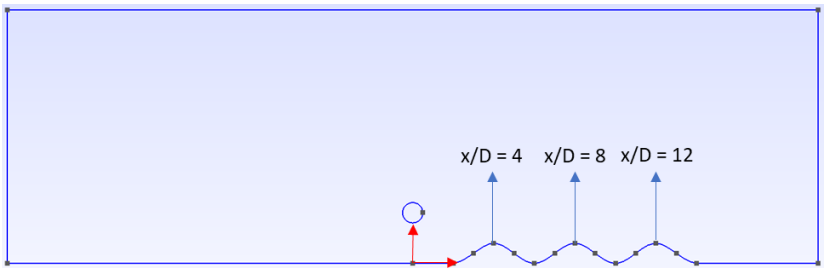

Figure 16- Velocity profile locations

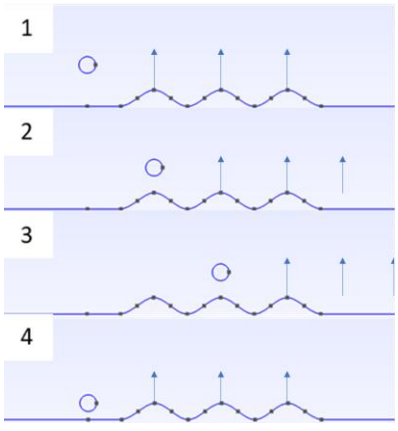

Figure 17- Velocity profile locations

Some observations to made from the Figure 18-20 are the similarities between case 2 and 3 which seem almost identical at *x/D* = 4. Case 4 seems nearly the same at each *x/D* location, while case 1 changes. Case 1 has an S-shaped profile which becomes stretched and the extrema come together the further downstream from the cylinder. Some conclusions to draw is that case 1 changes the further down stream but not greatly, case 2 and 3 changed after *x/D* = 4 but otherwise don't vary much, case 4 varies the least the further downstream and begins to accelerate in the upper half of the vertical coordinates for all locations.

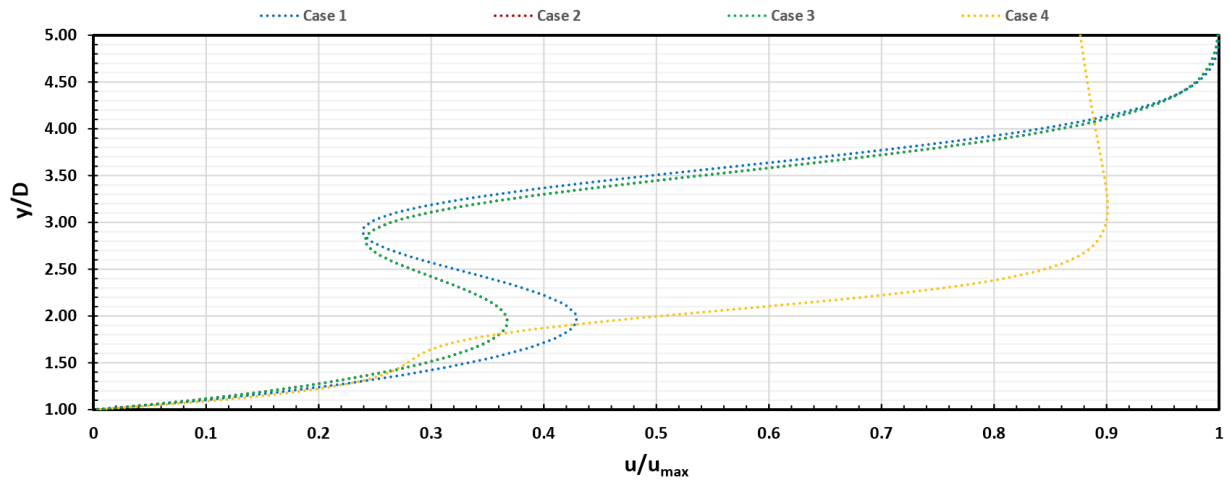

Figure 18- Velocity profiles at *x/D* = 4

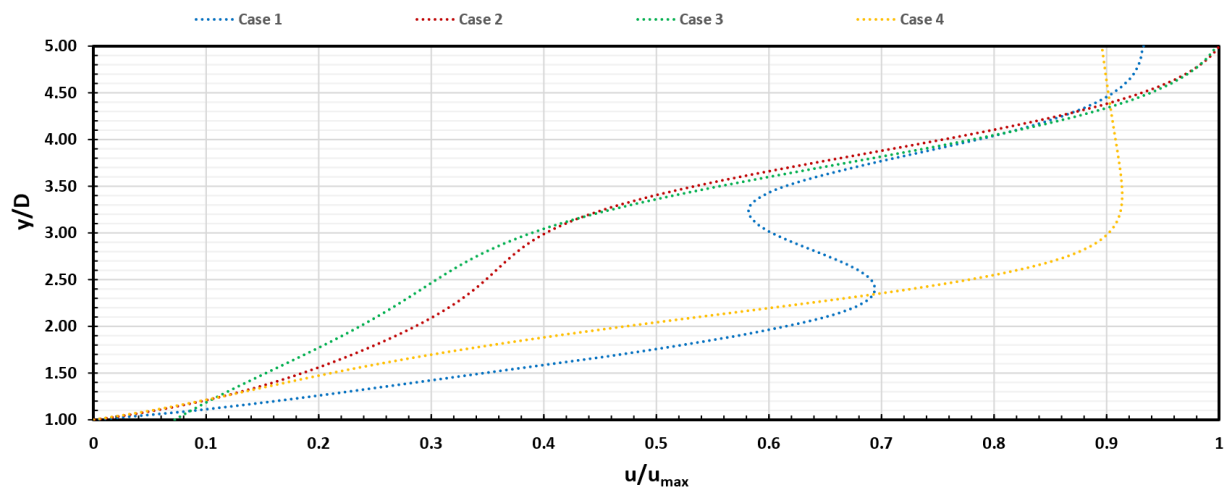

Figure 19- Velocity profile at *x/D* = 8

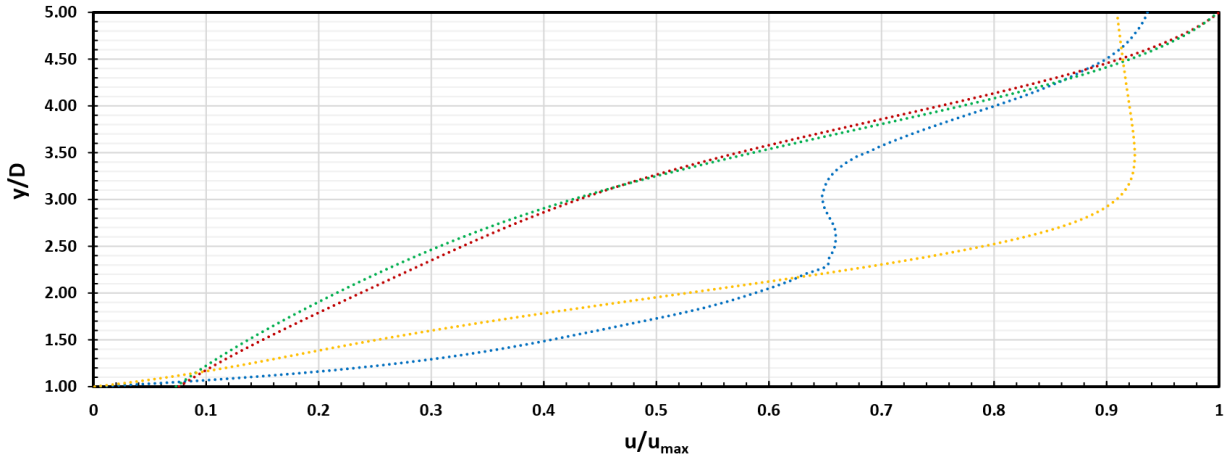

Figure 20- Velocity profile at *x/D* = 12

Eigenvalues

The results of the stability analysis will be displayed after the specified number of eigenvalues *nvec* converge and fall below the tolerance *evtol*. Figure 21 below displays the convergence for case 1 and the variables provided for each eigenvalue. These variables include the Magnitude, Angle, Growth rate, and frequency for each eigenvalue. These variables were calculated by Nektar using equations 1-4 below and the reverse can be done, using equation 5 the eigenvalues can be calculated from the magnitudes and angles.

```
Converged Eigenvalues: 5
          Magnitude   Angle       Growth      Frequency
EV:  0      187.07           0      10.463              0
EV:  1     1.05648    0.145555    0.109887    0.291111
EV:  2     1.05648   -0.145555    0.109887   -0.291111
EV:  3    0.990441    0.261647  -0.0192106    0.523294
EV:  4    0.990441   -0.261647  -0.0192106   -0.523294
```

Figure 21- Converged eigenvalues for case 1

$$\text{Magnitude: } M = |\lambda| \tag{1}$$

$$\text{Angle: } \theta = \arctan(\lambda_i/\lambda_r) \tag{2}$$

$$\text{Growth rate: } \sigma = \ln(M)/T \tag{3}$$

$$\text{Frequency: } \omega = \theta/T \tag{4}$$

$$\lambda_{r,i} = Me^{i\theta} \tag{5}$$

A contour plot of the streamwise component of the eigenmodes is shown in Figure 22 below, the corresponding real and imaginary part of the eigenvalue for each case is also labeled. The main observations are that the shape of the modes for flow past a cylinder is fairly similar to case 1 indicating the effect on stability is not significant. In addition, for case 4 the modes appear to curve and form an arc-like shape around the wavy ground.

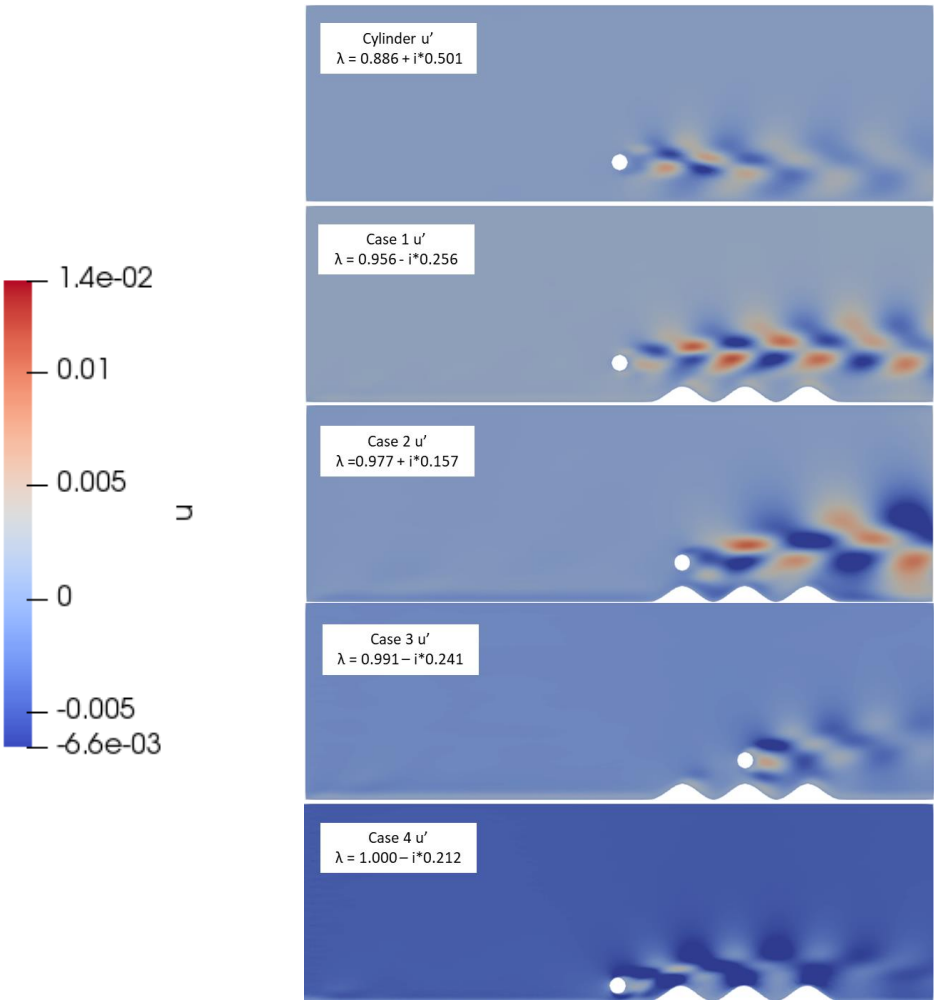

Figure 22- Contours of the streamwise component of the eigenmode (u')

The spanwise component of the eigenmodes are now shown in the contour plot below. Important features are noting that the shape of the eigenmodes become skewed upwards over the wavy ground at an angle while for flow past a cylinder and case 1 the modes remain nearly parallel with the upper boundary of the mesh.

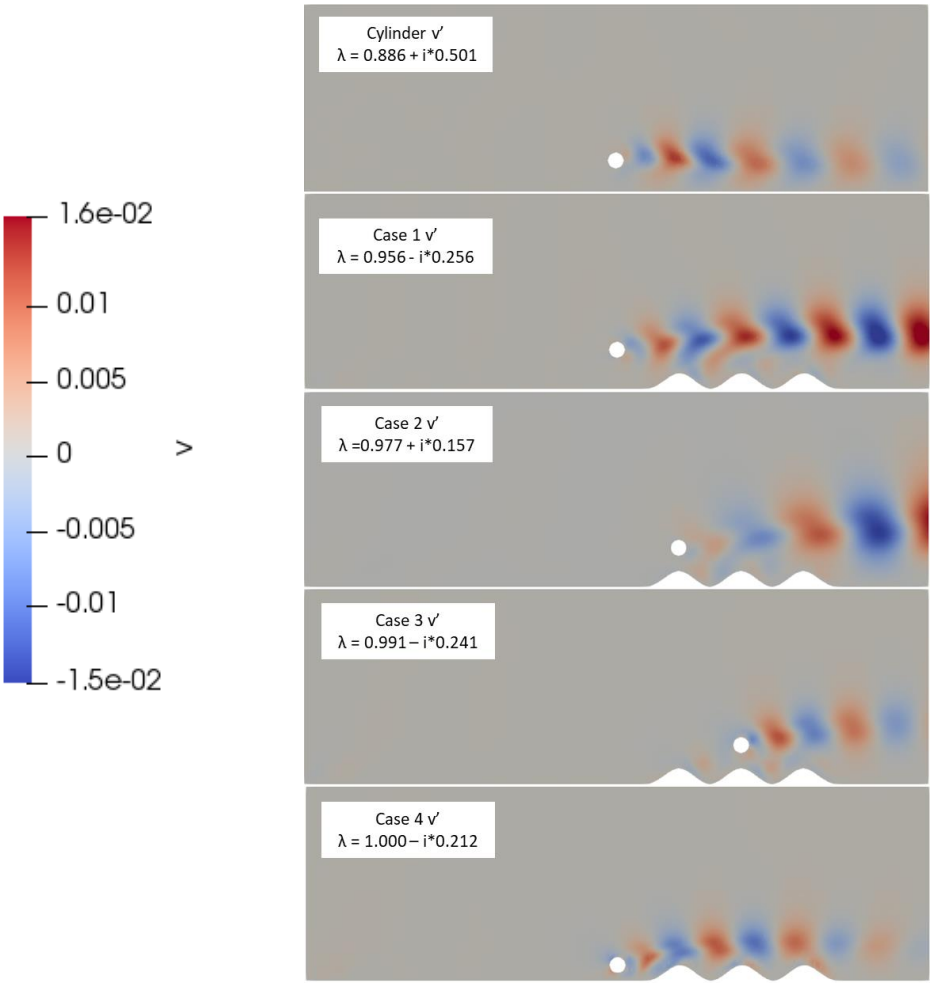

Figure 23- Contours of the spanwise component of the eigenmode (v')

The following two plots (Figure 24 and Figure *25*) show the value of the imaginary portion of the eigenvalue for the cylinder (case 0) and cases 1-4. The first plot below corresponds to the first eigenvalue, some observations are that the cylinder has the highest imaginary portion of the eigenvalue by far. The rest of the cases range in a value of 0.15 to 0.25. This large difference in values suggest change in the vortex shedding frequency as the imaginary portion of the eigenvalue of a system relates to frequency, the higher this value the higher the frequency.

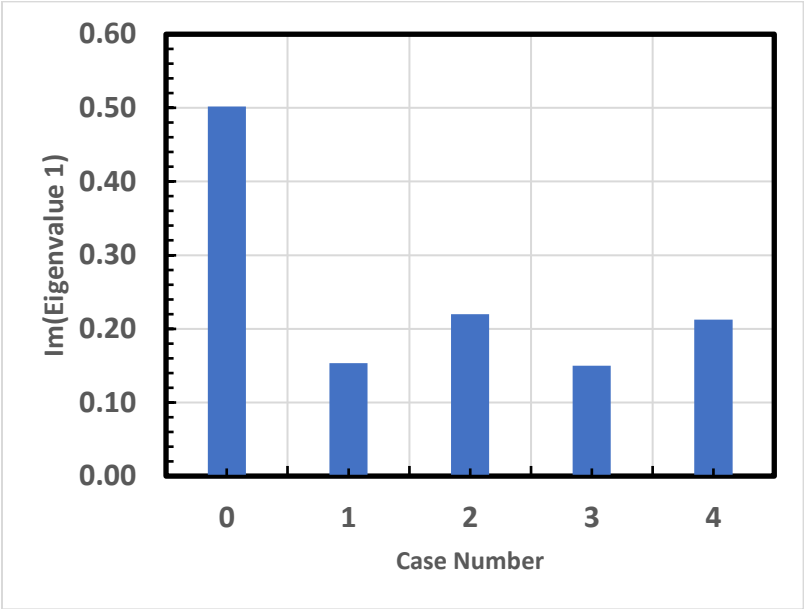

Figure 24- Eigenvalue 1 bar plot

For the second plot, the cylinder and case 4 have the same value as previously as only one eigenvalue was obtained for these cases for this study. These cases were nonetheless included in plot 2 in order to compare with the second eigenvalues for cases 1-3. The results are similar to the first eigenvalue with the cylinder having the highest value, it can again be concluded that the frequency changes when introducing a wavy ground.

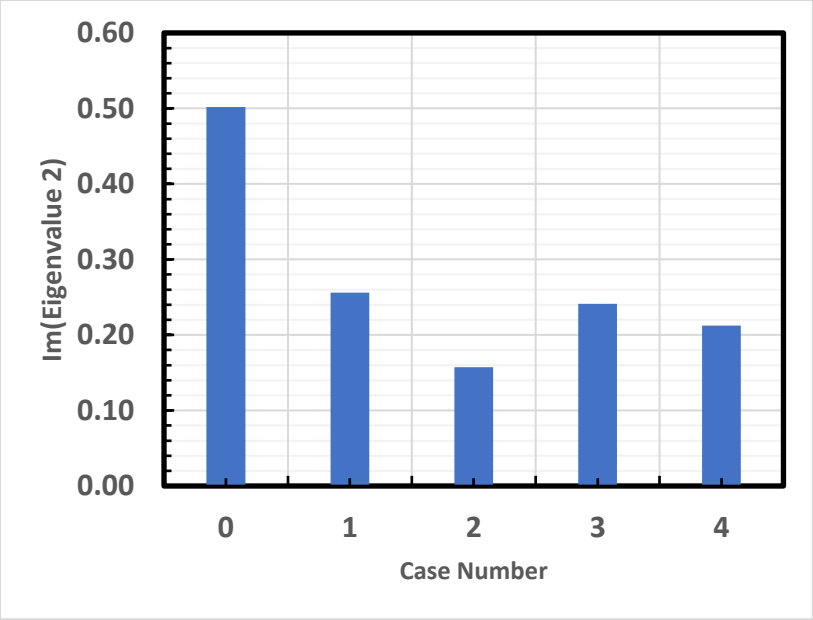

Figure 25- Eigenvalue 2 bar plot

CONCLUSIONS

Observations

The first significant observation to make is that the critical Reynolds number very clearly changes from the original plain flow past a cylinder. For cases 1-3 the critical Reynolds number is lowered from 30 to 25 and 20, for case 4 the critical Reynolds number is much higher at a value of 60. Additionally, the vortex shedding frequency from flow past a cylinder changed as the imaginary proportion of the eigen values differed, with a value of approximately 0.5 for the flow past the cylinder and values ranging from about 0.15 to 0.3 for cases 1-4. The last thing to note is that the shape of the eigenmodes changed from the flow past the cylinder, for cases 2 and 3 the eigenmodes became skewed and angled upwards as a result of the wavy ground.

Future work

To get a strong criterion for an accurate baseflow, a technique that can be applied in the future is to look for mesh convergence. This would entail increasing the order of the mesh being used from second order to third and checking the residuals to see whether they decrease by an order of magnitude, then repeating this for fourth and fifth order meshes. Other work that can be done in the future is to consider different geometries for the meshes. This would include other combinations of L/D and H/D or also changing the wavelength and amplitude of the wavy

ground which was kept constant for this study. Additionally, the number of peaks present in the wave like ground can be changed from three to have many more peaks. Ultimately, the same meshes need to be expanded into the third dimension to get full results that may apply in nature. The current simulations neglect significant effects that would need to be considered if the goal is to find real world applications.

REFERENCES

1. Yuan, F., Yu, W., & Lin, J. (2020). Numerical study of the effects of nanorod aspect ratio on Poiseuille flow and convective heat transfer in a circular minichannel. *Microfluidics and Nanofluidics*, *24*(8), 1–15.
2. C.D. Cantwell, D. Moxey, A. Comerford, A. Bolis, G. Rocco, G. Mengaldo, D. De Grazia, S. Yakovlev, J.-E. Lombard, D. Ekelschot, B. Jordi, H. Xu, Y. Mohamied, C. Eskilsson, B. Nelson, P. Vos, C. Biotto, R.M. Kirby, & S.J. Sherwin (2015). Nektar++: An open-source spectral/hp element framework. *Computer Physics Communications, 192, 205-219.*